

# UC Davis

## UC Davis Previously Published Works

### Title

Modeling subject-specific nonautonomous dynamics.

### Permalink

<https://escholarship.org/uc/item/0vn510mt>

### Journal

Statistica Sinica, 28(1)

### ISSN

1017-0405

### Authors

Zhou, Siyuan  
Paul, Debashis  
Peng, Jie

### Publication Date

2017

### DOI

10.5705/ss.202016.0113

Peer reviewed



Published in final edited form as:

*Stat Sin.* 2018 January ; 28(1): 423–447.

## Modeling subject-specific nonautonomous dynamics

Siyuan Zhou<sup>1</sup>, Debashis Paul<sup>2</sup>, and Jie Peng<sup>2</sup>

<sup>1</sup>The Meet Group, Inc

<sup>2</sup>University of California, Davis

### Abstract

We consider modeling non-autonomous dynamical systems for a group of subjects. The proposed model involves a common baseline gradient function and a multiplicative time-dependent subject-specific effect that accounts for phase and amplitude variations in the rate of change across subjects. The baseline gradient function is represented in a spline basis and the subject-specific effect is modeled as a polynomial in time with random coefficients. We establish appropriate identifiability conditions and propose an estimator based on the hierarchical likelihood. We prove consistency and asymptotic normality of the proposed estimator under a regime of moderate-to-dense observations per subject. Simulation studies and an application to the Berkeley Growth Data demonstrate the effectiveness of the proposed methodology.

### Keywords

Ordinary differential equation (ODE); gradient function; nonlinear mixed effects models; hierarchical likelihood; Levenberg-Marquardt method; phase variation

## 1 Introduction

Continuous-time smooth dynamical systems arise in modeling biological, physical, and chemical processes such as growth of organisms, synthesis of chemicals, disease progression, and dynamics of ecological systems. Many of these processes are modeled through systems of ordinary differential equations (ODEs). Most of the existing approaches assume known functional forms of the dynamical systems that are determined by a small number of parameters. Due to insufficient knowledge, sometimes a more flexible approach to modeling the gradient function of the dynamical system is necessary. Moreover, if observations are on a group of subjects, it may be beneficial to combine information across subjects. This can be achieved by including subject-specific effects into the model that

---

The Meet Group, Inc., San Francisco, CA.

zhousiyuan12@gmail.com

1 Shields Avenue, Department of Statistics, University of California, Davis, CA 95616

debpaull@ucdavis.edu

1 Shields Avenue, Department of Statistics, University of California, Davis, CA 95616

jjepeng@ucdavis.edu

Supplementary Materials

Supplementary Material, referred as such in the manuscript, contains details of proofs, additional figures, tables, and further simulation and data analysis results.

enable estimation of the population level dynamics while also estimating the dynamics for each individual. Mixed-effects models for ODEs have been used in pharmacokinetics (Li et al. (2002)) and in disease dynamics (Huang, Liu and Wu (2006); Guedj, Thiébaud and Commenges (2007); Huang and Lu (2008)), where the ODE is assumed to have a known parametric form. Recently, Wang et al. (2014) considered a semiparametric mixed-effects ODE model assuming a parametric ODE where the estimation is performed by imposing a penalty on the trajectories represented by splines.

In this paper, we model the dynamics for a group of subjects simultaneously by ordinary differential equations, with a common “baseline” dynamics depending on the current state and represented in a spline basis, and time-dependent subject-specific random effects that capture both amplitude and phase variation. The observed data for the  $i$ -th subject is the sample trajectory  $X_i(\cdot)$  measured at a set of time points in a finite time interval with measurement errors. In many studies, the rate of change  $X_i'(\cdot)$  is assumed to be a function of the state  $X_i(\cdot)$  alone, that is, the dynamics follows an autonomous system. However, many dynamics, especially those arising from biological systems, often display certain phase-variation in addition to amplitude-variation across subjects. This is prominent in the dynamics of human growth where some individuals start puberty earlier while for others the growth rate peaks at a later age. Since the defining feature of an autonomous system is that the rate of change at any given time is only a function of the state at that time, an autonomous system is inadequate in describing phase variations.

To model the phase variation in an interpretable way, we propose a system of nonautonomous ODEs where the gradient function is the product of two parts: a common time-independent fixed effects part (referred to as the *baseline gradient function*), and a time-dependent random effects part, capturing the phase and amplitude variations:

$X_i'(t) = e^{Z(t, \theta_i)} g(X_i(t))$ , where  $\theta_i$  is a random vector representing the unobserved subject-specific effects and  $Z(\cdot, \theta)$  is a function of time that captures both amplitude and phase variations. We represent the common gradient function  $g(\cdot)$  in a spline basis and model  $Z(t, \theta)$  as a polynomial in  $t$ . Decoupling of these two components requires an appropriate identifiability constraint that is discussed in Section 2. Moreover, to avoid singularity in the solution of the ODE, we also assume that  $g$  is either strictly positive or negative on its domain.

We propose an estimator based on the framework of hierarchical likelihood (Lee, Nelder and Pawitan (2006)). The model is fitted using the Levenberg-Marquardt nonlinear optimization procedure. The hierarchical likelihood-based estimation is computationally a much cheaper alternative to the commonly used maximum likelihood procedure for nonlinear mixed effects models (cf. Jiang (2007)) due to non-linearity in the ODEs and lack of closed form solutions. We adopt an asymptotic framework in which the baseline gradient function  $g$  is assumed to be exactly represented by a large but fixed number of basis functions, while for model fitting, we regularize  $g$  through adding a roughness penalty to the objective function. Under an appropriate identifiability constraint, we prove consistency of the proposed estimator of  $g$  when the measurements become dense within a time interval as the number of subjects  $n$  increases. We also prove that, when the number of measurements per subject

grows faster than  $\sqrt{n}$ , the proposed estimator has an asymptotic normal distribution. The latter result can be used to determine confidence sets for the baseline gradient function. We applied the proposed method to the Berkeley growth data and showed that valuable insights about human growth dynamics can be obtained through modeling the growth trajectories at a population level. The proposed method also provides an alternative framework for functional data analysis when such data are characterized by monotone sample trajectories.

Among related works, in Paul, Peng and Burman (2011) we considered a model with  $Z(t, \theta_i) = \theta_i$  to capture subject-specific amplitude variations in autonomous ODEs, even though no theoretical analysis was presented. The current proposal is seen as an extension of that model to nonautonomous ODEs. Also, in Paul, Peng and Burman (2016), we considered nonparametric estimation of  $g$  based on a single trajectory. Both the methodology and theoretical analysis presented in this paper are substantially different from that in Paul, Peng and Burman (2016).

The rest of the paper is organized as follows. The model is described in Section 2 and the model fitting procedure in Section 3. The asymptotic theory is established in Section 4. A simulation study is reported in Section 5 and the application to Berkeley growth data is described in Section 6. Proofs are given in the Appendix. Further details and additional numerical and graphical summaries are available in the Supplementary Material.

## 2 Model

In this section, we describe the proposed model and then discuss the identifiability constraint. We assume that the true trajectory  $X_i(\cdot)$ , corresponding to the  $i$ -th subject, follows the ODE:

$$X_i'(t) = e^{Z(t, \theta_i)} g(X_i(t)), \quad t \in [0, 1], \quad X_i(0) = a_i, \quad i = 1, \dots, n. \quad (1)$$

For simplicity of exposition, we treat the initial conditions  $a_i = X_i(0)$ ,  $i = 1, \dots, n$ , as known, though they can also be treated as random effects and estimated in a similar fashion as the  $\theta_i$ 's. We further assume that the baseline gradient function  $g$  in (1) is represented by a finite set of spline functions whose combined support covers the range of the observed trajectories:

$$g(x) = g_{\beta}(x) = \sum_{j=1}^M \beta_j \phi_j(x) \quad (2)$$

where  $\beta = (\beta_1, \dots, \beta_M)^T$  is unknown and  $\Phi(\cdot) = (\phi_1(\cdot), \dots, \phi_M(\cdot))^T$  is a set of spline functions. In this paper, we use a cubic B-spline basis with equally spaced knots and a large fixed  $M$ . Larger values of  $M$  provides a more accurate approximation to  $g$  while leading to higher variability of the estimator. To address this, we regularize  $g$  by adding a ridge-type roughness penalty term to the objective function (see (8)) to achieve bias-variance trade-off.

We model the subject-specific effect as a polynomial in  $t$  with random coefficients;

$$Z(t, \boldsymbol{\theta}_i) = \theta_{i1} + \theta_{i2}t + \cdots + \theta_{ip}t^{p-1}, \quad i=1, \dots, n, \quad (3)$$

with the working assumption that  $\boldsymbol{\theta}_i = (\theta_{i1}, \dots, \theta_{ip})^T \stackrel{i.i.d.}{\sim} N(\boldsymbol{\mu}_\theta, \boldsymbol{\Sigma}_\theta)$ ,  $\boldsymbol{\mu}_\theta = (\mu_1, \dots, \mu_p)^T$  and  $\boldsymbol{\Sigma}_\theta = \text{diag}(\sigma_{\theta_1}^2, \dots, \sigma_{\theta_p}^2)$  with  $\sigma_{\theta_k}^2 > 0$  for  $k = 1, \dots, p$ . Larger values of  $p$  increase model variability and consequently require a finer grid for numerically solving of the ODEs to overcome numerical instability. Instead of monomials in  $t$ , an orthogonal polynomial basis may be used to improve computational stability. The key feature of the random effect  $Z(t, \boldsymbol{\theta}_i)$  needed for theoretical derivations is that  $Z(t, \boldsymbol{\theta}_i)$  is linear in the parameter  $\boldsymbol{\theta}_i$ .

The observed data are modeled as

$$Y_{ij} = X_i(T_{ij}) + \varepsilon_{ij}, \quad j=1, \dots, m_i, \quad i=1, \dots, n, \quad (4)$$

with the working assumption that the  $\varepsilon_{ij}$ 's are i.i.d.  $N(0, \sigma_\varepsilon^2)$  and the  $T_{ij}$ 's are i.i.d. following a distribution with density  $f_T$  supported on  $[0, 1]$ . We also assume that the observational errors  $\varepsilon_{ij}$ 's and the random parameters  $\boldsymbol{\theta}_i$ 's are independent.

The model specified by (1), (2), and (3) is not identifiable without additional constraints, since the following transformation

$$\boldsymbol{\beta} \mapsto e^c \boldsymbol{\beta} \quad \text{and} \quad (\theta_{i1}, \dots, \theta_{ip}) \mapsto (-c + \theta_{i1}, \dots, \theta_{ip}), \quad c \in \mathbb{R}, \quad (5)$$

leaves the trajectories determined by the model invariant. This also suggests that a natural way to impose identifiability is to ensure that either the scale of  $\boldsymbol{\beta}$  or the mean of  $\boldsymbol{\theta}_{i1}$  is kept fixed at a given value. The constraint  $\mu_1 = \mathbb{E}(\boldsymbol{\theta}_{i1}) = 0$  is not effective in ensuring the asymptotic identifiability of the system, as can be seen from the asymptotic analysis in Section 4. We impose identifiability through the constraint

$$\sum_{j=1}^M \beta_j = 1. \quad (6)$$

In Section 4.2, we prove that (6), together with some technical conditions on the sampling design, ensures asymptotic identifiability of the parameters.

### 3 Model Fitting

A common approach to fitting mixed effects models is to integrate out the random effects and then maximize the resulting marginal likelihood with respect to the fixed effects. This

approach is computationally impractical here as it involves integrating out a random parameter (i.e.  $\{\theta_i\}_{i=1}^n$ ) in the solution of a nonlinear ODE that does not have an analytical form and can only be numerically evaluated. Instead, we adopt a hierarchical likelihood (henceforth, H-likelihood) approach (Lee, Nelder and Pawitan (2006)), which is a first-order approximation to the marginal likelihood. The H-likelihood approach involves specifying a working model for the distribution of random effects and then maximizing the resulting joint likelihood for the fixed and random effects. This can also be viewed as a penalized maximum likelihood procedure. For dense measurements, the H-likelihood based estimate of the fixed effects closely approximates the MLE or its second order approximation through Laplace's method (Jiang (2007)).

### 3.1 Penalized loss function

Let  $X_i(\cdot; \theta_i, \beta)$  denote the solution to (1) with the gradient function  $g(\cdot) \equiv g_{\beta}(\cdot)$  specified in (2) and  $Z(\cdot, \theta_i)$  specified in (3). Then the negative joint log likelihood of the observed data  $\mathbf{Y} = (Y_{ij}; 1 \leq i \leq n; 1 \leq j \leq m_i)$  and the random effects  $\Theta = (\theta_1, \dots, \theta_n)$  is given by, up to multiplicative and additive constants,

$$\sum_{i=1}^n \sum_{j=1}^{m_i} \ell_{ij}(\theta_i, \beta),$$

with,  $\ell_{ij}(\theta_i, \beta) = (Y_{ij} - X_i(t_{ij}; \theta_i, \beta))^2 + \sigma_{\varepsilon}^2 (\theta_i - \mu_{\theta})^T \Sigma_{\theta}^{-1} (\theta_i - \mu_{\theta}) / m_i.$  (7)

The trajectory  $X_i(\cdot; \theta_i, \beta)$  and its gradients with respect to  $\theta_i$  and  $\beta$  can be numerically computed using the Runge-Kutta method, as described in Paul, Peng and Burman (2011).

In order to achieve a bias-variance trade-off and higher computational stability, we use a fixed large  $M$  and impose a roughness penalty on  $g$  of the form  $\lambda_{\beta} \int_{d_0}^{d_1} (g''(x))^2 dx$ . Here  $[d_0, d_1]$  is the range covered by the trajectories and  $\lambda_{\beta} \geq 0$  is a penalty parameter. This formulation is related to penalized spline regression (Ruppert (2002); Yu and Ruppert (2002)). Under (2), we have

$$\int_{d_0}^{d_1} (g''(x))^2 dx = \beta^T \mathbf{H} \beta, \quad \text{with} \quad \mathbf{H} = \int_{d_0}^{d_1} \Phi''(x) (\Phi''(x))^T dx$$

where  $\Phi(x) = (\phi_1(x), \dots, \phi_M(x))^T$ . Then the penalized loss function is

$$L(\theta, \beta) = \sum_{i=1}^n \sum_{j=1}^{m_i} \ell_{ij}(\theta_i, \beta) + \lambda_{\beta} \beta^T \mathbf{H} \beta. \tag{8}$$

The proposed estimator is

$$(\hat{\boldsymbol{\theta}}, \hat{\boldsymbol{\beta}}) := \underset{(\boldsymbol{\theta}, \boldsymbol{\beta})}{\operatorname{argmin}} L(\boldsymbol{\theta}, \boldsymbol{\beta}), \text{ subject to } \sum_k \beta_k = 1. \quad (9)$$

The estimator of the gradient function  $g$  is then  $\hat{g}(x) = \sum_{j=1}^M \hat{\beta}_j \phi_j(x)$ , and estimated trajectories  $X_i$ 's can be evaluated by solving (1) with  $\boldsymbol{\theta}_i$ 's replaced by  $\hat{\boldsymbol{\theta}}_i$ 's and  $g$  replaced by  $\hat{g}$ .

### 3.2 Fitting algorithm

We use the Levenberg-Marquardt algorithm for nonlinear regression (Nocedal and Wright (2006)) to minimize (8). It involves iteratively updating  $\boldsymbol{\theta}_i$ 's and  $\boldsymbol{\beta}$ . At each step, we need to evaluate  $X_i(\cdot; \boldsymbol{\theta}_i, \boldsymbol{\beta})$  and its partial derivatives with respect to  $\boldsymbol{\theta}_i$  and  $\boldsymbol{\beta}$ . Since these are not available in close forms, a 4<sup>th</sup> order Runge-Kutta method is used to evaluate these functions on a fine grid. More details are given in the Supplementary Material.

Let  $\boldsymbol{\theta}_i^c$  and  $\boldsymbol{\beta}^c$  denote the current estimates of  $\boldsymbol{\theta}_i$  and  $\boldsymbol{\beta}$  at each updating step of the Levenberg-Marquardt algorithm. Then  $\mu_k$  is estimated as the mean of the  $\theta_{ik}^c$ 's. The variances  $\sigma_k^2$ 's and  $\sigma_\varepsilon^2$  can be viewed as either unknown parameters or as tuning parameters. In the former case, they are estimated as the empirical variances of the  $\theta_{ik}^c$ 's and the current residuals  $\tilde{\varepsilon}_{ij} = Y_{ij} - X_i(t_{ij}; \boldsymbol{\theta}_i^c, \boldsymbol{\beta}^c)$ , respectively. In the latter case, these parameters can be selected, similarly as the penalty parameter  $\lambda_\beta$ , through cross validation. The penalty parameter  $\lambda_\beta$  controls the trade-off between fidelity to the data and the complexity of the model. We use an approximate leave-one-subject-out cross-validation score  $\widehat{CV}$  for choosing  $\lambda_\beta$ , described in Section S.6 of the Supplementary Material.

## 4 Asymptotic theory

In this section, we present results on the asymptotic behavior of the proposed estimator of the baseline gradient function  $g$  under the model specified by (1) – (4). For simplicity of exposition, let  $\phi_1, \dots, \phi_M$  be the B-spline basis functions of degree 3, with equally spaced knots, and combined support  $[d_0, d_1]$ . The asymptotic theory remains valid for any well-conditioned basis with twice continuously differentiable basis functions supported on this interval. In order to avoid singularity in the solution of the ODE, we assume throughout that  $g$  is either strictly positive or strictly negative on its domain.

Throughout we assume that the initial conditions are randomly distributed and known. In order to simplify the derivations, we treat  $\boldsymbol{\mu}_\theta = \mathbb{E}(\boldsymbol{\theta}_i)$  as known and, without loss of generality, equal to zero. If the mean  $\boldsymbol{\mu}_\theta$  is unknown, additional terms in the expression for the Fisher information with respect to  $\boldsymbol{\beta}$  result, which can be neglected asymptotically under assumptions **A1–A4** and **F1** (see Sections 4.1 and 4.2), as indicated in Section S.3.1 of the Supplementary Material.

We establish consistency and asymptotic normality of the proposed estimator  $\hat{\boldsymbol{\beta}}$  of  $\boldsymbol{\beta}$  under the identifiability constraint (6). For consistency, we assume that the  $m_i$ 's, the numbers of

measurements per subject, increase to infinity uniformly as the sample size  $n$  increases. For asymptotic normality, we further assume that  $\min_{1 \leq i \leq n} m_i$  grows faster than  $\sqrt{n}$ . The asymptotic theory presented here differs from the standard theory of nonlinear mixed effects models (cf. Jiang (2007)) due to the use of H-likelihood estimator rather than marginal likelihood estimator, and the imposition of the identifiability constraint on  $\beta$ . Proofs of the asymptotic results make use of the profile H-likelihood with respect to  $\beta$ , where the profiling is done by substituting  $\theta_i$ 's by their local optimizers as a function of  $\beta$ .

#### 4.1 Assumptions

- A0** The true parameter  $\beta_0$  satisfies  $\sum_{k=1}^M \beta_{k,0} = 1$ , and  $g_{\beta_0}(x) > 0$  for all  $x \in (d_0, d_1)$ .
- A1** The distribution  $F_{\theta}$  of the  $\theta_i$ 's and the distribution  $F_a$  of the  $a_i$ 's have bounded support.
- A2** The measurement times  $T_{ij}$  are randomly distributed on  $[0, 1]$  with a density  $f_T$  that is bounded above and below (away from zero). Also, the noise  $\varepsilon_{ij}$  are i.i.d.  $N(0, \sigma_\varepsilon^2)$ .
- A3** Let  $\underline{m} = \min_{1 \leq i \leq n} m_i$  and  $\bar{m} = \max_{1 \leq i \leq n} m_i$ . Then  $\underline{m} \rightarrow \infty$  as  $n \rightarrow \infty$  so that  $\bar{m}/\underline{m}$  remains bounded.

Condition **A0** reduces one degree of freedom in the parameter and can always be achieved through a recentering of  $\theta_{j1}$ . Condition **A1** helps to ensure the boundedness of the trajectories and their derivatives. Moreover, **A0** and a refinement of conditions **A0** and **A1** (condition **F1** in Section A.1) are needed to prove that the Fisher information matrix (19) associated with the profile H-likelihood with respect to  $\beta$  is nonsingular (see Section 4.2). The latter ensures asymptotic identifiability of the model. Conditions **A2** and **A3** can be replaced by assuming that the observations are on a regular grid with grid spacings converging to zero as  $n \rightarrow \infty$ . The assumption on the  $\varepsilon_{ij}$ 's can be relaxed to that they are i.i.d. sub-Gaussian random variables.

#### 4.2 Asymptotic identifiability

We present a detailed analysis of asymptotic identifiability. The identifiability condition (6) allows us to reparametrize  $\beta$  as

$$\beta = \beta(\gamma) := M^{-1} \mathbf{1}_M + \mathbf{C}\gamma, \quad \gamma \in \mathbb{R}^{M-1}, \quad (10)$$

where  $\mathbf{C}$  is an  $M \times (M-1)$  matrix satisfying  $\mathbf{C}^T \mathbf{1}_M = \mathbf{0}$  and  $\text{rank}(\mathbf{C}) = M-1$ .

Due to the reparametrization of  $\beta$ , given by (10), we express the likelihood function and its derivatives as a function of  $\gamma$ . Let  $\gamma_0$  and  $\theta_i^*$  denote the true parameters, and the  $a_i$ 's denote the (true) initial conditions. In the following, we suppress the dependence of the trajectories on the initial conditions  $a_i$  since these are treated as known.

Define the *negative penalized log H-likelihood* for the  $i$ -th subject by



$$L_i^H(\boldsymbol{\theta}_i, \boldsymbol{\gamma}) = \frac{1}{2} \left( \sum_{j=1}^{m_i} (Y_{ij} - X(T_{ij}; \boldsymbol{\theta}_i, \boldsymbol{\beta}(\boldsymbol{\gamma})))^2 + \boldsymbol{\theta}_i^T \Psi^{-1} \boldsymbol{\theta}_i + \frac{\lambda}{n} \boldsymbol{\beta}(\boldsymbol{\gamma})^T \mathbf{H} \boldsymbol{\beta}(\boldsymbol{\gamma}) \right) \quad (11)$$

where  $\Psi = (1/\sigma_\varepsilon^2) \sum_{\rho}$ . Here,  $L_i^H(\boldsymbol{\theta}_i, \boldsymbol{\gamma}) = \frac{1}{2} \left( \sum_{j=1}^{m_i} \ell_{ij}(\boldsymbol{\theta}_i, \boldsymbol{\beta}(\boldsymbol{\gamma})) + \frac{\lambda}{n} \boldsymbol{\beta}(\boldsymbol{\gamma})^T \mathbf{H} \boldsymbol{\beta}(\boldsymbol{\gamma}) \right)$ , where  $\ell_{ij}$  is as in (7) with  $\boldsymbol{\mu}_\theta = 0$ .

Due to the lack of convexity of  $L_i^H(\boldsymbol{\theta}_i, \boldsymbol{\gamma})$  with respect to  $\boldsymbol{\theta}_i$ , in general the value of  $\boldsymbol{\theta}_i$  minimizing this function for a given  $\boldsymbol{\gamma}$  is not unique. Therefore, throughout, we take

$$\hat{\boldsymbol{\theta}}_i(\boldsymbol{\gamma}) = \arg \min_{\boldsymbol{\theta}_i \in \mathcal{B}(\boldsymbol{\theta}_i^*, \rho_n)} L_i^H(\boldsymbol{\theta}_i, \boldsymbol{\gamma}), \quad (12)$$

where  $\rho_n = O(\log n)^{-2}$  and  $\mathcal{B}(\boldsymbol{\theta}_i^*, \rho_n) = \{\boldsymbol{\theta}_i \in \mathbb{R}^p : \|\boldsymbol{\theta}_i - \boldsymbol{\theta}_i^*\| \leq \rho_n\}$ . Thus,  $\hat{\boldsymbol{\theta}}_i(\boldsymbol{\gamma})$  is a local minimizer of  $L_i^H(\boldsymbol{\theta}_i, \boldsymbol{\gamma})$  given  $\boldsymbol{\gamma}$  that is also a global minimizer within a radius  $\rho_n$  of the true  $\boldsymbol{\theta}_i^*$ . See Remark 1 for obtaining an initial estimate of  $\boldsymbol{\theta}_i$  that satisfies this. The “estimator”  $\hat{\boldsymbol{\theta}}_i(\boldsymbol{\gamma})$  can be shown to be uniformly close to  $\boldsymbol{\theta}_i^*$  when  $\boldsymbol{\gamma}$  is within a suitably small distance of  $\boldsymbol{\gamma}_0$  (see (A.8) for details). Define the *negative profile log H-likelihood* for  $\boldsymbol{\gamma}$  by

$$L^P(\boldsymbol{\gamma}) = \sum_{i=1}^n L_i^P(\boldsymbol{\gamma}), \quad \text{where } L_i^P(\boldsymbol{\gamma}) := L_i^H(\hat{\boldsymbol{\theta}}_i(\boldsymbol{\gamma}), \boldsymbol{\gamma}), \quad i=1, \dots, n,$$

and  $\hat{\boldsymbol{\theta}}_i(\boldsymbol{\gamma})$  is as in (12). Henceforth, we treat  $L_i^P$  interchangeably as a function of  $\boldsymbol{\gamma}$  or  $\boldsymbol{\beta}$ .

We now discuss the asymptotic identifiability of the model. Let  $q(t) = (1, t, \dots, t^{p-1})$  so that  $Z(t, \boldsymbol{\theta}) = \boldsymbol{\theta}^T q(t)$ . Let

$$\Xi^{11}(a, \boldsymbol{\theta}, \boldsymbol{\beta}) = \int_0^1 (X^\beta(t; a, \boldsymbol{\theta}, \boldsymbol{\beta})) (X^\beta(t; a, \boldsymbol{\theta}, \boldsymbol{\beta}))^T f_T(t) dt \quad (13)$$

$$\Xi^{12}(a, \boldsymbol{\theta}, \boldsymbol{\beta}) = \int_0^1 (X^\beta(t; a, \boldsymbol{\theta}, \boldsymbol{\beta})) (X^\theta(t; a, \boldsymbol{\theta}, \boldsymbol{\beta}))^T f_T(t) dt \quad (14)$$

$$\Xi^{22}(a, \boldsymbol{\theta}, \boldsymbol{\beta}) = \int_0^1 (X^\theta(t; a, \boldsymbol{\theta}, \boldsymbol{\beta})) (X^\theta(t; a, \boldsymbol{\theta}, \boldsymbol{\beta}))^T f_T(t) dt, \quad (15)$$

where  $X(t; a, \boldsymbol{\theta}, \boldsymbol{\beta})$  denotes the solution to the equation

$$x'(t) = e^{\theta^T q(t)} g_{\beta}(x(t)), \quad t \in [0, 1], \quad x(0) = a, \quad (16)$$

and  $X^{\beta} := \frac{\partial}{\partial \beta} X$  and  $X^{\theta} = \frac{\partial}{\partial \theta} X$ .

We add a (mild) additional assumption.

**A4** For all  $\beta$  in a neighborhood  $\mathcal{B}$  of  $\beta_0$ , and all  $(a, \theta) \in \text{supp}(F_a \times F_{\theta})$ , the minimum eigenvalue of  $\Xi^{22}(a, \theta, \beta)$  is bounded below by some constant  $c > 0$ .

We take

$$\Xi^{1|2}(a, \theta, \beta) = \Xi^{11}(a, \theta, \beta) - \Xi^{12}(a, \theta, \beta) \Xi^{22}(a, \theta, \beta)^{-1} \Xi^{12}(a, \theta, \beta)^T; \quad (17)$$

$$\tilde{G}(a, \theta, \gamma) = C^T \Xi^{1|2}(a, \theta, \beta(\gamma)) C. \quad (18)$$

We also make a slight refinement of **A0** and **A1**, stated as condition **F1** in Section A.1, that ensures that if  $\beta$  is in a neighborhood of  $\beta_0$ , then the combined support of the basis functions  $\{\phi_1, \dots, \phi_M\}$  is covered by trajectories corresponding to suitably chosen pairs  $(a_i, \theta_i)$ .

Now, we can deduce that (details given in Section A.1) the matrix

$$\mathcal{G}(\gamma) = \int \tilde{G}(a, \theta, \gamma) dF_a(a) dF_{\theta}(\theta) \quad (19)$$

is well-conditioned. Since  $\mathcal{G}(\gamma)$  is the integrated Fisher information matrix of the profile H-likelihood  $L^P(\gamma)$  for  $\gamma$ , this is equivalent to the asymptotic identifiability of  $\gamma$ , as closeness in terms of the values of the objective function implies closeness in terms of the values of  $\gamma$ , due to the well-conditioning of  $\mathcal{G}(\gamma)$ .

### 4.3 Consistency and Asymptotic Normality

We prove consistency of the estimator of  $\beta$  (equivalently,  $g$ ) by showing that under the identifiability constraint (6), and assuming that the roughness penalty parameter  $\lambda \equiv \lambda_{\beta}$  is sufficiently small, there is a sequence of local minimizers of the loss function (8) that converges in probability to the true  $\beta_0$  as  $n \rightarrow \infty$ . We also determine its rate of convergence and prove its asymptotic normality after appropriate centering and scaling. We introduce the notation  $\tilde{O}$  to mean that if  $X_n = \tilde{O}(c_n)$  then given any  $C > 0$ , there exists  $C' > 0$  such that  $|X_n/c_n - C'|$  with probability at least  $1 - n^{-C}$  for all  $n$ .

We make an assumption about the density of measurements.

**A5** There is a  $\delta_0 > 0$  such that  $\liminf_{n \rightarrow \infty} \underline{m} n^{-\delta_0} > 0$  where  $\underline{m} = \min_i m_i$ .

This condition ensures that in a Taylor expansion of the loss function with respect to the parameters, terms beyond quadratics can be ignored asymptotically.

**Remark 1**—A good initial estimate for the parameters is helpful for convergence of the algorithm. We can obtain an initial estimate for each  $\theta_j$  by a simple two-stage method consisting of first obtaining nonparametric smoothers for  $X_i(\cdot)$  and  $X_i'(\cdot)$  for each  $i$ , then using the expansion

$$\log \hat{X}_i'(T_{ij}) = q(T_{ij})^T \theta_i + \log g(\hat{X}_i(T_{ij})) + \delta_{ij}, \quad j=1, \dots, m_i, \quad (20)$$

where  $q(t) = (1, t, \dots, t^{p-1})^T$  and the  $\delta_{ij}$ 's are approximation errors, to estimate  $\theta_i$  through regression, while treating  $\log g$  as an arbitrary smooth function. It can be shown that, under the identifiability restriction and conditions **A1–A5** and **F1**, the estimators  $\tilde{\theta}_i$  thus obtained satisfy  $\max_{1 \leq i \leq n} \|\tilde{\theta}_i - \theta_i^*\| = o_p(\rho_n)$ , where  $\rho_n$  is as in (12).

**Theorem 1:** *Suppose that **A0–A5** and **F1** are satisfied and  $\lambda = o(\sqrt{n})$ . Then there exists a root  $\hat{\gamma}$  of the equation  $\frac{d}{d\gamma} L^P(\gamma) = 0$  that is a local minimizer of  $L^P(\gamma)$  and satisfies*

$$\|\hat{\gamma} - \gamma_0\| = O_p \left( \max \left\{ \frac{1}{\sqrt{n\bar{m}}}, \frac{1}{\bar{m}} \right\} \right). \quad (21)$$

Clearly, (21) also implies that

$$\|\hat{\beta} - \beta_0\| = O_p \left( \max \left\{ \frac{1}{\sqrt{n\bar{m}}}, \frac{1}{\bar{m}} \right\} \right). \quad (22)$$

The basic strategy of the proof is as follows. For a small  $\alpha_n > 0$ , we compare the value of  $L^P(\gamma_0 + \alpha_n \delta)$ , where  $\delta$  is a unit vector in  $\mathbb{R}^{M-1}$ , with that of  $L^P(\gamma_0)$ . Our goal is to show that, for an appropriately chosen sequence  $\alpha_n \rightarrow 0$ , we have

$$\mathbb{P} \left( \inf_{\delta \in \mathbb{R}^{M-1}} L^P(\gamma_0 + \alpha_n \delta) > L^P(\gamma_0) \right) \rightarrow 1. \quad (23)$$

We choose the sequence  $\alpha_n$  to be a constant multiple of  $\max \{ (\log n)^{1/2} (n\bar{m})^{-1/2}, 1/\bar{m}, \lambda/n \}$ .

This also establishes the existence of a root  $\hat{\gamma}$  of  $\frac{d}{d\gamma} L^P(\gamma) = 0$  within a radius of  $\alpha_n$  around  $\gamma_0$ . The result (21) is obtained by expanding  $\frac{d}{d\gamma} L^P(\hat{\gamma})$  around  $\gamma_0$  in a Taylor series and thereby obtaining an asymptotic representation of  $\hat{\gamma}$ . The details are given in the Appendix.

We also prove asymptotic normality of the estimator of  $\boldsymbol{\gamma}$  by imposing a stronger condition on the rate of growth of  $m_i$ 's.

$$\mathbf{A5}' \quad \underline{m} = \min_i m_i \gg (\log n)^6 n^{1/2} \text{ as } n \rightarrow \infty.$$

**Theorem 2:** Suppose that **A0–A4**, **A5'** and **F1** are satisfied and  $\lambda = o(\sqrt{n})$ . Let

$N_n = \sum_{i=1}^n m_i$ . Then there exists a root  $\hat{\boldsymbol{\gamma}}$  of the equation  $\frac{d}{d\boldsymbol{\gamma}} L^P(\boldsymbol{\gamma}) = 0$  that satisfies

$$\sqrt{N_n}(\hat{\boldsymbol{\gamma}} - \boldsymbol{\gamma}_0 - \Gamma_n(\boldsymbol{\gamma}_0)^{-1} \mathbf{b}_n(\boldsymbol{\gamma}_0)) \Rightarrow N(0, \sigma_\varepsilon^2 \Gamma(\boldsymbol{\gamma}_0)^{-1}), \quad (24)$$

where  $\mathbf{b}_n(\boldsymbol{\gamma}_0)$  is a stochastic bias term of the form

$$\mathbf{b}_n(\boldsymbol{\gamma}_0) = \frac{1}{N_n} \sum_{i=1}^n \sum_{\ell=1}^4 \mathbf{C}^T f_\ell(a_i, \boldsymbol{\theta}_i^*, \boldsymbol{\gamma}_0), \quad (25)$$

with  $\{f_\ell(a_i, \boldsymbol{\theta}_i^*, \boldsymbol{\gamma}_0)\}_{\ell=1}^4$  as given by (S.1)–(S.4) in the Supplementary Material, and

$$\Gamma_n(\boldsymbol{\gamma}_0) = \frac{1}{N_n} \sum_{i=1}^n m_i \tilde{G}(a_i, \boldsymbol{\theta}_i^*, \boldsymbol{\gamma}_0), \quad (26)$$

and  $\Gamma(\boldsymbol{\gamma}_0) := \lim_{n \rightarrow \infty} \Gamma_n(\boldsymbol{\gamma}_0)$ , assuming the limit exists in probability. If this limit exists in probability only along a subsequence, then the limit in (24) holds along the same subsequence.

The proof of Theorem 2 is in the Appendix.

**Remark 2—**If the  $m_i$ 's are i.i.d. following a distribution (indexed by  $n$ ) supported on  $[\underline{m}, \bar{m}]$ , independent of  $(\boldsymbol{\theta}_i, \{\varepsilon_{ij}\})$ , and **A5'** holds, then  $\Gamma(\boldsymbol{\gamma}_0)$  in (26) exists almost surely and is the integrated Fisher information  $\mathcal{I}(\boldsymbol{\gamma}_0)$  (see equation (19)).

**Remark 3—**The term  $\Gamma_n(\boldsymbol{\gamma}_0)^{-1} \mathbf{b}_n(\boldsymbol{\gamma}_0)$  is a bias term that is of the order  $O_P(\underline{m}^{-1})$ . This term results from the nonlinearity of  $X(t; a_i, \boldsymbol{\theta}_i, \boldsymbol{\beta})$  with respect to  $\boldsymbol{\theta}_i$ . If the measurements per subject are sufficiently dense, then this term can be neglected in (24).

**Remark 4—**By Theorem 2, the asymptotic variance of  $\hat{\boldsymbol{\gamma}}$  is  $\sigma_\varepsilon^2 \Gamma_n(\boldsymbol{\gamma}_0)^{-1}$ . We estimate  $\sigma_\varepsilon^2$  by

$$\hat{\sigma}_\varepsilon^2 = \frac{1}{df} \sum_{i=1}^n \sum_{j=1}^{m_i} (Y_{ij} - \hat{X}_{ij}(\hat{\boldsymbol{\beta}}))^2 \quad (27)$$

where  $df_n := \sum_{i=1}^n (m_i - p) - M = N_n - np - M$  is the degrees of freedom (since  $\theta_j$  is  $p$ -dimensional and  $\beta$  is  $M$ -dimensional). We can also estimate  $\Gamma_n(\gamma_0)$  and  $b_n(\gamma_0)$  from data, as is shown in Section S.1 of the Supplementary Material.

## 5 Simulation Study

In this section, we report on the finite sample performance of the proposed methodology in estimating the gradient functions and the trajectories. We also examine the implications of mis-specification of the subject-specific effect components  $Z(\cdot; \theta_j)$ .

We refer to the true baseline gradient function  $g$  used here as the “two-peak” function according to its shape. The “two-peak” gradient function  $g$  and some random realizations of the trajectories following model (1) are depicted in Figure S.1 in the Supplementary Material. The chosen  $g$  is not exactly representable by a finite number of cubic B-spline functions with equally spaced knots, though the accuracy of approximation improves with more knots.

We considered two different sampling rates: (i) *sparse*: 3–8 measurements per trajectory/subject; and (ii) *dense*: 30–50 measurements per trajectory/subject. For each setting, we generated  $n = 25$  sample trajectories. We set the subject-specific functions  $Z(\cdot, \theta_j)$  as linear functions in  $t$ . For the *dense* case, the random parameters  $\theta_j$ 's were i.i.d. Normal with  $\mu_\theta = (0, 2)$  and  $\Sigma_\theta = \text{diag}(0.1^2, 0.2^2)$ . For the *sparse* case,  $\mu_\theta = (0, 0)^T$  and  $\mu_\theta = (0, 2)^T$ , with the variance  $\Sigma_\theta$  the same as in the *dense* case. Measurement errors  $\varepsilon_{ij}$ 's were i.i.d.  $N(0, \sigma_\varepsilon^2)$ . For the *sparse* case, we set  $\sigma_\varepsilon = 0.01$ . For the *dense* case, we took  $\sigma_\varepsilon = 0.01$  and  $\sigma_\varepsilon = 0.02$ . For each scenario, 500 independent replicates were generated.

In the fitting procedure, we used  $M$  cubic B-spline basis functions with equally spaced knots on the combined range of the observed trajectories. We chose  $M = 30$  to allow a high degree of flexibility in representing  $g$ . Twenty values of the roughness penalty parameter  $\lambda_\beta$  over an appropriate range were considered and the “optimal” value  $\lambda_{\beta, \text{opt}}$  was selected by the approximate leave-one-subject-out cross validation score  $\widehat{CV}$ . We used  $\hat{g}$  and  $\{\hat{X}_i(\cdot)\}_{i=1}^n$  to denote the estimates of the baseline gradient function and sample trajectories, respectively, corresponding to  $\lambda_{\beta, \text{opt}}$ . We also used the true model with  $p = 2$  for the subject-specific effect  $Z(\cdot; \theta_j)$  and allowed up to 5000 iterations in the Levenberg-Marquardt algorithm.

For performance evaluation, we report summary statistics of integrated squared error (ISE) of gradient functions estimation and trajectories estimation, denoted by  $ISE(\hat{g})$  and  $ISE(\hat{X})$ , respectively, across the 500 independent replicates. In order to simultaneously evaluate the estimated gradient functions across all subjects, we define

$$ISE(\hat{g}) := \int_0^1 (e^{\hat{\mu}(t)} \hat{g}(\hat{X}(t)) - e^{\mu(t)} g(\bar{X}(t)))^2 dt,$$

where  $\hat{\mu}(t) = \sum_{k=1}^p \hat{\mu}_k t^{k-1}$  is the estimated mean subject-specific effect,  $\bar{X}(t) = n^{-1} \sum_{i=1}^n X_i(t)$  is the mean of the true sample trajectories, and  $\hat{\bar{X}}(t) = n^{-1} \sum_{i=1}^n \hat{X}_i(t)$  is the mean of the estimated sample trajectories. We use the function  $e^{\mu(t)} g(\bar{X}(t))$  as the benchmark so as to capture the variability in estimation of  $g$  and the  $\theta_j$ 's simultaneously. This function also reflects the derivative of  $X_i(t)$  averaged across subjects and thus can be seen as an overall measure of the rate of growth. Finally,  $ISE(\hat{X})$  is defined as  $n^{-1} \sum_{i=1}^n \int_0^1 (\hat{X}_i(t) - X_i(t))^2 dt$ .

Estimation accuracy of the gradient functions and the trajectories, based on 500 independent replicates for each scenario, is summarized in Table 1, where  $\widehat{CV}$  was used for selecting the penalty parameter  $\lambda_\beta$ . We report the mean, standard deviation (SD), median and median absolute deviation (MAD) of  $ISE(\hat{g})$  and  $ISE(\hat{X})$ . These results show that there is a substantial improvement in performance when the sampling rate is increased from the sparse case to the dense case. Compare these results with those in Table S.1 of the Supplementary Material. The latter reports the results based on the minimization of  $ISE(\hat{g})$ . The median  $ISE(\hat{g})$  under  $\widehat{CV}$  is within a factor of two to that under “ideal” model selection and the difference is smaller in the dense case. In terms of trajectory estimation, there is little difference in terms of median  $ISE(\hat{X})$  between these two model selection criteria.

In Figure 1, we depict the estimated gradient functions under the dense case with  $\sigma_e = 0.01$ . On the left panel, we plot the point-wise 5% and 95% percentiles and mean of the function  $\hat{g}(x) := s_\beta \hat{g}(x)$ , along with the true  $g(x)$ , against  $x$ , across 500 independent replicates. Here,  $s_\beta := \sum_{j=1}^M \beta_j^{tr}$  and  $(\beta_j^{tr})_{j=1}^M$  is the set of basis coefficients of the projected  $g$  onto the  $M = 30$  B-spline basis functions with equally spaced knots used in the model fitting procedure.

Rescaling by  $s_\beta$  is to account for the scaling in  $\hat{g}$  due to the constraint  $\sum_{j=1}^M \beta_j = 1$ . On the right panel, we plot the point-wise 5% and 95% percentiles and mean of the function  $e^{\hat{\mu}(t)} \hat{g}(\hat{\bar{X}}(t))$ , along with the point-wise mean of  $e^{\mu(t)} g(\bar{X}(t))$ , all treated as a function of the mean of  $\bar{X}(t)$ . These plots demonstrate that the gradient function estimation is quite accurate and captures the shape of the true gradient functions. The estimation under all the other cases are depicted in Figures S.2, S.3 and S.4 of the Supplementary Material. The summary for  $ISE(\hat{g}) := \int (s_\beta \hat{g}(x) - g(x))^2 dx$ , treating  $\hat{g}(x) = s_\beta \hat{g}(x)$  as an estimator of  $g(x)$ , is reported in Table S.2 of the Supplementary Material.

We also investigated the impact of misspecification of the subject-specific effects  $Z(\cdot; \theta_j)$ 's on the estimation accuracy. We used  $p_{tr}$  to denote the true order of the  $Z(\cdot; \theta_j)$ 's, took  $p_{tr} = 1$  and  $p_{tr} = 2$ , and generated data under the sparse and dense sampling rates for each of the two models. We again used the “Two-peak” function as the true baseline gradient function, and had  $n = 25$  subjects. The hyperparameters were  $\mu_\theta = 0$  and  $\Sigma_\theta = 0.1^2$  when  $p_{tr} = 1$ , and  $\mu_\theta = (0, 0)^T$  (for sparse), or  $\mu_\theta = (0, 2)^T$  (for dense) and  $\Sigma_\theta = \text{diag}(0.1^2, 0.2^2)$  when  $p_{tr} = 2$ . In all settings, the error variance was  $\sigma_\varepsilon^2 = 0.01^2$ . In the fitting procedure, we used  $M = 30$

cubic B-spline basis functions with equally spaced knots and considered  $p = 1$  and  $p = 2$  for both models,  $p_{tr} = 1$  and  $p_{tr} = 2$ .

We report  $ISE(\hat{g})$ , using  $p = p_{tr}$  and the “ideal” model selection for  $\lambda_\beta$ , and  $ISE(\hat{g})$ , and using  $\widehat{CV}$  for the selection of both  $\lambda_\beta$  and  $p$ , in Tables S.3 and S.4, respectively, in the Supplementary Material.  $\widehat{CV}$  tends to select larger  $p$ , as is evidenced by the fact that in at least 95% of the cases the larger model ( $p = 2$ ) is selected regardless of  $p_{tr}$ . However, when  $p_{tr} = 2$ , the model with  $p = 1$  produces significantly biased estimation and inflated ISE (results not reported). When  $p_{tr} = 1$ , using the model with  $p = 2$  results in a reasonably good fit. Specifically, the median ISE under  $\widehat{CV}$  is within a factor of three of the median  $ISE(\hat{g})$  under the “ideal” case where  $p_{tr}$  is used in model fitting. Moreover, the difference in  $ISE(\hat{g})$  between  $\widehat{CV}$  and the “ideal” case decreases as the sampling rate increases. These results show that when the models are nested, although  $\widehat{CV}$  tends to select larger models, the proposed method is still reliable in terms of estimating the gradient function, especially for relatively dense observations. Additional model selection results are reported in Section S.8 of the Supplementary Material.

## 6 Application to Berkeley growth data

We applied the proposed method to the *Berkeley Growth Data* (Tuddenham and Snyder (1954)). This data set consists of measurements of heights (in centimeters) of 54 female and 39 male subjects, measured at 31 time points (same for all subjects) from the age of 1 to 18 years. Our aim was to estimate the population level common growth dynamics as well as individual dynamics using the proposed methodology.

Many statistical analyses have been done to describe the features of human growth. A popular approach is curve alignment based on estimation of time-warping functions, including landmark registration (Gasser et al. (1991)), continuous monotone registration (Ramsay and Li (1998)), “self-modeling” registration (Gervini and Gasser (2004)). Many parametric models have been proposed for describing postnatal growth in humans, for example, Jenss and Bayley (1937) and Count (1943) for early childhood growth, and Preece and Baines (1978), Bock et al. (1973), and Hauspie et al. (1980) for adolescent growth by logistic and the Gompertz functions. Several models have been proposed to fit individual trajectories at different age intervals (see Hauspie, Cameron and Molinari (2004) for an overview). Growth velocities, at the level of individual subjects, for various age groups, have also been analyzed nonparametrically by Gasser et al. (1984) and Gasser et al. (1985).

One important difference of these works from the proposed method is that they primarily focus on fitting individual growth trajectories rather than estimating the common growth dynamics. Our method has the advantage of providing a description of the dynamics at a population level while isolating subject-specific phase and amplitude variations. Thus our approach contributes to enhancing the understanding of common patterns and variations of human growth in a population.

We first carried out a preliminary study to understand the nature of the growth dynamics. We plotted the empirical derivatives, denoted by  $Y'(t)$ , computed by taking successive divided

differences, against the observed heights  $Y(t)$ , across all individuals (Figure S.5 in the Supplementary Material). The empirical gradient shows that the growth rate decreases rapidly at an early age. Around a mean height of 145cm, the female growth rate peaks again, while the male growth rate reaches a peak at a mean height of around 160cm, before slowly decreasing to nearly zero at about 160cm for female and 180cm for male subjects.

We made several small modifications in the fitting procedure to improve its stability and accuracy. First, to improve the fit at an early age and thereby reduce the boundary effect, we linearly extrapolated each trajectory for age below one year. Also, since the rate of growth nearly vanishes beyond a certain height, we forced the baseline gradient  $g$  to be close to zero for large  $x$  by adding a tail penalty of the form

$$\lambda_R \int_A^{200} g(x)^2 dx = \lambda_R \beta^T \left[ \int_A^{200} \phi(x) \phi(x)^T dx \right] \beta,$$

where  $\lambda_R > 0$  and  $0 < A < 200$  were selected by  $\widehat{CV}$ . To improve convergence of the algorithm, we fixed  $\mu_k = \mathbb{E}(\theta_{ik})$  at zero for  $k > 1$ .

We used  $M = 15$  cubic B-splines with equally spaced knots. We considered three models with constant ( $p = 1$ ) (autonomous model), linear ( $p = 2$ ) and quadratic ( $p = 3$ ) random effects  $Z(\cdot, \theta)$ . Since the estimates are not very sensitive to the specification of the variance of the random effects  $\Sigma_\theta$  after preliminary studies, we set  $\Sigma_\theta$  to be diagonal with diagonal elements  $(\sigma_{\theta_k}^2)_{k=1}^p$ , with each  $\sigma_{\theta_k} = 5$ . We also set the error variance  $\sigma_\varepsilon^2$  at 0.25. Initial conditions  $a_i$ 's were treated as known and equal to the value of each (extrapolated) trajectory at time zero. We used  $\widehat{CV}$  to choose various model parameters including  $\lambda_\beta, p, A, \lambda_R$ . The selected models have  $p = 3$  for both genders and have  $(A, \lambda_R) = (175, 1000)$  for the female group, and  $(A, \lambda_R) = (190, 500)$  for the male group.

Observed and fitted growth trajectories (under the selected model with  $p = 3$ ) are plotted in Figure S.7 of the Supplementary Material which shows good fits for the selected models. In addition, the MISEs between the fitted and observed trajectories with quadratic subject-specific effects ( $p = 3$ ) improve upon those with the linear subject-specific effect ( $p = 2$ ) by 57.55% (female) and 38.69% (male), respectively, and improve upon those with constant subject-specific effect ( $p = 1$ , autonomous model) by 75.74% (female) and 61.67% (male), respectively. Residual plots of the trajectory fits against time, under  $p = 1, 2, 3$ , given in Figure S.8 of the Supplementary Material, show improvements in trajectory fitting with model larger order (i.e., larger  $p$ ). We also considered the model with  $p = 4$ . Although it tends to have even smaller MISE and slightly less spread out residuals, since it yields very similar estimate of the gradient function as under  $p = 3$ , we place the detailed results under this setting in Section S.8 of the Supplementary Material.

Plots of the fitted gradient function  $e^{Z(t, \hat{\mu}_0)} \hat{g}(\widehat{X}(t))$  against the mean observed trajectory  $\widehat{X}(t)$  for  $p = 3$  are shown in Figure 2. Notably, both females and males have more prominent growth spurts than suggested by the empirical growth dynamics in Figure S.5. Moreover,



fitted individual growth rates  $\hat{X}'_i(t)$  versus  $t$  and versus the fitted trajectory  $\hat{X}(t)$ , respectively, depicted in Figure S.6 in the Supplementary Material, clearly show both phase and amplitude variations.

## 7 Discussion

We propose a flexible approach to modeling a collection of trajectories through ordinary differential equations with subject-specific effects. Our model has a time varying multiplicative random effect component capturing phase and amplitude variations in the trajectories, and a fixed baseline gradient function reflecting population level common dynamics. We implement an estimation procedure through the hierarchical likelihood framework and provide a detailed asymptotic theory. The proposed method can be used to extract both phase and amplitude variations in the dynamics in an interpretable manner, as is shown by the application to the Berkeley growth data. A nontrivial extension of the theory would be to the setting where the baseline gradient function is treated nonparametrically. The method can also be extended to model dynamics of multivariate trajectories and data involving covariates.

## Supplementary Material

Refer to Web version on PubMed Central for supplementary material.

## Acknowledgments

We thank the Editor, an associate editor and the referee for their constructive suggestions. This research is partially supported by NSF grants DMS-10-07583, DMS-11-06690, DMS-14-07530 and NIH grant 1R01EB021707.

## References

- Bock RD, Wainer H, Petersen A, Thissen D, Murray J, Roche A. A parameterization for individual human growth curves. *Human Biology*. 1973; 45:63–80. [PubMed: 4694175]
- Count EW. Growth patterns of the human physique: an approach to kinetic anthropometry: Part I. *Human Biology*. 1943; 15:1–32.
- Gasser T, Kneip A, Binding A, Prader A, Molinari L. The dynamics of linear growth in distance, velocity and acceleration. *Annals of Human Biology*. 1991; 18:187–205. [PubMed: 1877807]
- Gasser T, Müller HG, Köhler W, Molinari L, Prader A. Nonparametric regression analysis of growth curves. *The Annals of Statistics*. 1984; 12:210–229.
- Gasser T, Müller HG, Köhler W, Prader A, Largo R, Molinari L. Velocity and acceleration of height growth using kernel estimation. *Annals of Human Biology*. 1985; 12:129–138. [PubMed: 3985567]
- Gervini D, Gasser T. Self-modelling warping functions. *Journal of the Royal Statistical Society: Series B*. 2004; 66:959–971.
- Guedj J, Thiébaud R, Commenges D. Maximum likelihood estimation in dynamical models for HIV. *Biometrics*. 2007; 63:1198–1206. [PubMed: 17489970]
- Hauspie, RC., Cameron, N., Molinari, L. *Methods in Human Growth Research*. Vol. 39. Cambridge University Press; 2004.
- Hauspie RC, Wachholder A, Baron G, Cantraine F, Susanne C, Graffar M. A comparative study of the fit of different functions to longitudinal data of growth in height of Belgian girls. *Annals of Human Biology*. 1980; 7:347–358. [PubMed: 7436348]
- Huang Y, Liu D, Wu H. Hierarchical Bayesian methods for estimation of parameters in a longitudinal HIV dynamic system. *Biometrics*. 2006; 62:413–423. [PubMed: 16918905]

- Huang Y, Lu T. Modeling long-term longitudinal HIV dynamics with application to an AIDS clinical study. *The Annals of Applied Statistics*. 2008; 2:1384–1408.
- Jenss RM, Bayley N. A mathematical method for studying the growth of a child. *Human Biology*. 1937; 9:556–563.
- Jiang, J. *Linear and Generalized Linear Mixed Models and Their Applications*. Springer; New York: 2007.
- Lee, Y., Nelder, JA., Pawitan, Y. *Generalized Linear Models with Random Effects: Unified Analysis via H-likelihood*. CRC Press; 2006.
- Li L, Brown MB, Lee KH, Gupta S. Estimation and inference for a spline enhanced population pharmacokinetic model. *Biometrics*. 2002; 58:601–611. [PubMed: 12229995]
- Nocedal, J., Wright, S. *Numerical Optimization*. Springer; New York: 2006.
- Paul D, Peng J, Burman P. Semiparametric modeling of autonomous nonlinear dynamical systems with application to plant growth. *The Annals of Applied Statistics*. 2011; 5:2078–2108.
- Paul D, Peng J, Burman P. Nonparametric estimation of dynamics of monotone trajectories. *The Annals of Statistics*. 2016; 44:240–2432.
- Preece MA, Baines MJ. A new family of mathematical models describing the human growth curve. *Annals of Human Biology*. 1978; 5:1–24. [PubMed: 646321]
- Ramsay JO, Li X. Curve registration. *Journal of the Royal Statistical Society: Series B*. 1998; 60:351–363.
- Ruppert D. Selecting the number of knots for penalized splines. *Journal of Computational and Graphical Statistics*. 2002; 11:735–757.
- Tuddenham, RD., Snyder, MM. *Publications in child development*. Vol. 1. University of California; Berkeley: 1954. Physical growth of California boys and girls from birth to eighteen years; p. 183
- Wang L, Cao J, Ramsay JO, Burger DM, Laporte CJL, Rockstroh JK. Estimating mixed-effects differential equation models. *Statistics and Computing*. 2014; 24:111–121.
- Yu Y, Ruppert D. Penalized spline estimation for partially linear single-index models. *Journal of the American Statistical Association*. 2002; 97:1042–1054.

## Appendix

### A.1 Nonsingularity of observed Fisher information

We make the following assumption that is a slight refinement of **A0** and **A1**. To state it, we let  $\text{supp}(\Phi)$  be the set  $\cup_{j=1}^M \text{supp}(\phi_j)$ .

**F1** There exists an integer  $K \geq 1$  (not depending on  $n$  and  $m_j$ 's), nonoverlapping intervals  $A_1, \dots, A_K \subset \text{supp}(F_a)$ , and a set  $\Theta_0 \subset \text{supp}(F_\theta)$  such that,

1.  $\mathbb{P}(a \in A_k) > 0$  for all  $k$ , and  $\mathbb{P}(\theta \in \Theta_0) > 0$ ;
2. if  $p > 1$ , then for all  $\theta \in \Theta_0$ ,  $\theta_j = 0$  for some  $j \in \{2, \dots, p\}$ , where  $\theta_j$  denotes the  $j$ -th coordinate of  $\theta$ ;
3. if  $(a_{i_k}, \theta_{i_k}) \in A_k \times \Theta_0$  for  $k = 1, \dots, K$ , and  $\beta$  is in a fixed neighborhood of  $\beta_0$ , then the ranges of  $X(t; a_{i_k}, \theta_{i_k}, \beta)$  for successive  $k$ 's intersect, and one of the following holds:
  - a.  $\cup_{k=1}^K \{X(t; a_{i_k}, \theta_{i_k}, \beta) : t \in [0, 1]\} \supseteq \text{supp}(\Phi)$ ;
  - b.  $\cup_{k=1}^K \{X(t; a_{i_k}, \theta_{i_k}, \beta) : t \in [0, 1]\} \supseteq B_\Phi$  where the interval  $B_\Phi \subseteq \text{supp}(\Phi)$  is such that  $\int_{B_\Phi} \phi_j(x) dx = 1$  for all  $j = 1, \dots, M$ .

Condition 3(b) in **F1** is easily satisfied through proper choice of  $B_\Phi$  and appropriate renormalization of  $\{\phi_j\}_{j=1}^M$ .

We write  $\mathbf{i} \in \mathcal{Q}_0$  to indicate that the set of indices  $\mathbf{i} = (i_1, \dots, i_K)$  is such that  $a_{i_k} \in A_k$  and  $\boldsymbol{\theta}_{i_k} \in \Theta_0$  for all  $k$ . Define, for a set of indices  $\mathbf{i} \in \{1, \dots, n\}$ ,

$$\tilde{G}_i(\boldsymbol{\gamma}) = \sum_{k=1}^K \tilde{G}(a_{i_k}, \boldsymbol{\theta}_{i_k}, \boldsymbol{\gamma}).$$

We first show that for any  $\mathbf{i} \in \mathcal{Q}_0$ , the matrix  $\tilde{G}_i(\boldsymbol{\gamma})$  is nonsingular, whenever  $\boldsymbol{\gamma}$  (correspondingly,  $\boldsymbol{\beta}$ ) lies in an appropriate fixed neighborhood of  $\boldsymbol{\gamma}_0$  (correspondingly,  $\boldsymbol{\beta}_0$ ) and satisfies conditions **A0**, **A1**, **A4**, and **F1**. In the following we establish that the smallest eigenvalue of  $\tilde{G}_i$ , for  $\mathbf{i} \in \mathcal{Q}_0$ , is a positive-valued random variable.

The matrix  $\tilde{G}_i(\boldsymbol{\gamma})$  is singular if and only if there exists a nonzero vector  $\mathbf{h}$ , such that  $\mathbf{h}^T \tilde{G}_i(\boldsymbol{\gamma}) \mathbf{h} = 0$ . This condition can be expressed as

$$0 = \sum_{k=1}^K \mathbf{h}^T \mathbf{C}^T G(a_{i_k}, \boldsymbol{\theta}_{i_k}, \boldsymbol{\beta}(\boldsymbol{\gamma})) \mathbf{C} \mathbf{h} \\ = \sum_{k=1}^K \left[ \int_0^1 (\mathbf{h}^T \mathbf{u}_k(t))^2 f_T(t) dt - \left( \int_0^1 \mathbf{h}^T \mathbf{u}_k(t) \mathbf{v}_k(t) f_T(t) dt \right) \left( \int_0^1 \mathbf{v}_k(t) \mathbf{v}_k(t)^T f_T(t) dt \right)^{-1} \left( \int_0^1 \mathbf{h}^T \mathbf{u}_k(t) \mathbf{v}_k(t) f_T(t) dt \right)^T \right]$$

where  $\mathbf{u}_k(t) = \mathbf{C}^T X^\beta(t; a_{i_k}, \boldsymbol{\theta}_{i_k}, \boldsymbol{\beta}(\boldsymbol{\gamma}))$  and  $\mathbf{v}_k(t) = X^\theta(t; a_{i_k}, \boldsymbol{\theta}_{i_k}, \boldsymbol{\beta}(\boldsymbol{\gamma}))$ . Therefore, using a standard argument from multivariate linear regression, by treating the  $\mathbf{u}_k(t)$  as responses,  $\mathbf{v}_k(t)$  as predictors and using the least squares principle, we conclude that there exist  $p \times 1$  vectors  $\{\mathbf{d}_{i_k}\}_{k=1}^K$  such that

$$\sum_{k=1}^K \int_0^1 \left[ \mathbf{h}^T \mathbf{C}^T X_i^\beta(t; a_{i_k}, \boldsymbol{\theta}_{i_k}, \boldsymbol{\beta}(\boldsymbol{\gamma})) - \mathbf{d}_{i_k}^T X_i^\theta(t; a_{i_k}, \boldsymbol{\theta}_{i_k}, \boldsymbol{\beta}(\boldsymbol{\gamma})) \right]^2 f_T(t) dt = 0. \tag{A.1}$$

This is equivalent to the following condition: for all  $k = 1, \dots, K$ ,

$$\mathbf{h}^T X_i^\gamma(t; a_{i_k}, \boldsymbol{\theta}_{i_k}, \boldsymbol{\beta}(\boldsymbol{\gamma})) = \mathbf{h}^T \mathbf{C}^T X_i^\beta(t; a_{i_k}, \boldsymbol{\theta}_{i_k}, \boldsymbol{\beta}(\boldsymbol{\gamma})) = \mathbf{d}_{i_k}^T X_i^\theta(t; a_{i_k}, \boldsymbol{\theta}_{i_k}, \boldsymbol{\beta}(\boldsymbol{\gamma})). \tag{A.2}$$

Under the reparametrization (10), using (16), we have

$$\begin{aligned}
g_{\beta(\boldsymbol{\gamma})}(x) &= \boldsymbol{\beta}(\boldsymbol{\gamma})^T \Phi(x) = \boldsymbol{\gamma}^T \mathbf{C}^T \Phi(x) + M^{-1} \mathbf{1}_M^T \Phi(x) =: \tilde{g}_{\boldsymbol{\gamma}}(x) \\
X_i'(t) &= e^{\boldsymbol{\theta}_i^T q(t)} \tilde{g}_{\boldsymbol{\gamma}}(X_i(t)) = e^{\boldsymbol{\theta}_i^T q(t)} (\boldsymbol{\gamma}^T \mathbf{C}^T \Phi(X_i(t)) + M^{-1} \mathbf{1}_M^T \Phi(X_i(t))) \\
\frac{d}{dt}(X_i \boldsymbol{\theta}(t)) &= e^{\boldsymbol{\theta}_i^T q(t)} \tilde{g}_{\boldsymbol{\gamma}}(X_i(t)) \frac{\partial X_i(t)}{\partial \boldsymbol{\theta}} + e^{\boldsymbol{\theta}_i^T q(t)} \tilde{g}_{\boldsymbol{\gamma}}(X_i(t)) q(t)
\end{aligned} \tag{A.3}$$

$$\frac{d}{dt}(X_i \boldsymbol{\gamma}(t)) = e^{\boldsymbol{\theta}_i^T q(t)} \tilde{g}_{\boldsymbol{\gamma}}(X_i(t)) \frac{\partial X_i(t)}{\partial \boldsymbol{\gamma}} + e^{\boldsymbol{\theta}_i^T q(t)} \mathbf{C}^T \Phi(X_i(t)). \tag{A.4}$$

Differentiating (A.2) with respect to  $t$ , and combining with (A.3) and (A.4),

$$\mathbf{h}^T \mathbf{C}^T \Phi(X_{i_k}(t)) = g_{\beta(\boldsymbol{\gamma})}(X_{i_k}(t)) \mathbf{d}_{i_k}^T q(t), \quad k=1, \dots, K, \quad t \in [0, 1]. \tag{A.5}$$

Here  $q(t)$  is a vector of monomials of  $t$  of dimension  $p$ ,  $\mathbf{d}_{i_k} \in \mathbb{R}^p$ , and the functions  $\phi_j$ 's are piecewise polynomials. From this, it can be checked that (A.5) holds only if  $\mathbf{d}_{i_k}^T q(t) = c_k$  for all  $k$ , where the  $c_k$ 's do not depend on  $t$  (see Section S.2 of the Supplementary Material for detail). By **F1**, the  $c_k$ 's must all be equal since the sets  $\{X_{i_k}(t) | t \in [0, 1]\}$  overlap for successive  $k$ . Without loss of generality,  $c_1 = \dots = c_K = 1$ . Again by **F1**, we conclude that either,  $(\mathbf{C}(\mathbf{h} - \boldsymbol{\gamma}) - M^{-1} \mathbf{1}_M)^T \Phi(x) = 0$  for all  $x \in \text{supp}(\Phi)$  (under **F1.3(a)**), or  $(\mathbf{C}(\mathbf{h} - \boldsymbol{\gamma}) - M^{-1} \mathbf{1}_M)^T \Phi(x) = 0$  for all  $x \in B_{\Phi}$  (under **F1.3(b)**). Consequently, in either case,

$$\mathbf{1}_M^T \mathbf{C}(\mathbf{h} - \boldsymbol{\gamma}) = M^{-1} \mathbf{1}_M^T \mathbf{1}_M = 1.$$

The left side of this equation is 0 since  $\mathbf{1}_M^T \mathbf{C} = 0$ , and the right side is 1. This contradiction proves that there does not exist a vector  $\mathbf{h}$  such that  $\mathbf{h}^T \tilde{\mathbf{G}}_i(\boldsymbol{\gamma}) \mathbf{h} = 0$ , which implies that  $\tilde{\mathbf{G}}_i(\boldsymbol{\gamma})$  is non-singular.

## A.2 Proof of Theorem 1

Some of the proof details are deferred to the Supplementary Material. Throughout, we use  $\boldsymbol{\theta}_i^*$  to denote the true value of  $\boldsymbol{\theta}_i$  and drop the reference to the initial value  $a_i$  that is assumed to be known. We use  $\boldsymbol{\beta}(\boldsymbol{\gamma})$  to mean  $\boldsymbol{\beta}$ , where  $\boldsymbol{\beta}(\boldsymbol{\gamma}) = \mathbf{C}\boldsymbol{\gamma} + M^{-1} \mathbf{1}_M$ . Also, we use  $\hat{\boldsymbol{\theta}}_i(\boldsymbol{\beta})$  and  $\hat{\boldsymbol{\theta}}_i(\boldsymbol{\gamma})$  interchangeably.

The basic building block is an asymptotic expansion of the restricted optimizer  $\hat{\boldsymbol{\theta}}_i(\boldsymbol{\gamma})$  (see (A.12)). Let  $\mathbb{E}_T$  denote the expectation with respect to  $T \sim f_T$ . Take

$$\begin{aligned}
\mathcal{L}(\boldsymbol{\theta}, \boldsymbol{\gamma} | \boldsymbol{\theta}_i^*) &= \mathbb{E}_T (X(T; \boldsymbol{\theta}, \boldsymbol{\beta}) - X(T; \boldsymbol{\theta}_i^*, \boldsymbol{\beta}_0))^2, \\
\text{and } \hat{\boldsymbol{\theta}}_i(\boldsymbol{\beta}) \equiv \hat{\boldsymbol{\theta}}_i(\boldsymbol{\gamma}) &= \arg \min_{\boldsymbol{\theta} \in \mathcal{B}(\boldsymbol{\theta}_i^*, \rho_n)} \mathcal{L}(\boldsymbol{\theta}, \boldsymbol{\gamma} | \boldsymbol{\theta}_i^*),
\end{aligned}$$

where  $\rho_n$  and  $\mathcal{B}(\theta_i^*, \rho_n)$  are as in the definition (12) of  $\hat{\theta}_i(\boldsymbol{\gamma})$ . Using the fact that  $\mathcal{L}(\theta_i^*, \boldsymbol{\gamma}_0 | \theta_i^*) = 0$  and  $\theta_i^*$  is a global minimum of  $\mathcal{L}(\boldsymbol{\theta}, \boldsymbol{\gamma}_0 | \theta_i^*)$ , it follows, through a Taylor expansion, that uniformly on  $\mathcal{B}(\theta_i^*, \rho_n)$

$$\begin{aligned} \mathcal{L}(\boldsymbol{\theta}, \boldsymbol{\gamma} | \theta_i^*) &= \frac{1}{2}(\boldsymbol{\theta} - \theta_i^*)^T \nabla_{\boldsymbol{\theta}\boldsymbol{\theta}^T} \mathcal{L}(\theta_i^*, \boldsymbol{\gamma}_0 | \theta_i^*)(\boldsymbol{\theta} - \theta_i^*) \\ &+ O(\|\boldsymbol{\theta} - \theta_i^*\|^3) + O(\|\boldsymbol{\theta} - \theta_i^*\| \|\boldsymbol{\gamma} - \boldsymbol{\gamma}_0\|) + O(\|\boldsymbol{\gamma} - \boldsymbol{\gamma}_0\|^2). \end{aligned} \quad (\text{A.6})$$

From (A.6), we deduce that  $\|\bar{\theta}_i(\boldsymbol{\gamma}) - \theta_i^*\| = O(\|\boldsymbol{\gamma} - \boldsymbol{\gamma}_0\|)$  and that  $\bar{\theta}_i(\boldsymbol{\gamma})$  satisfies  $\nabla_{\boldsymbol{\theta}} \mathcal{L}(\boldsymbol{\theta}, \boldsymbol{\gamma} | \theta_i^*)|_{\boldsymbol{\theta} = \bar{\theta}_i(\boldsymbol{\gamma})} = 0$ . Using standard arguments, we can now show that under the conditions of Theorem 1, as long as  $\|\boldsymbol{\gamma} - \boldsymbol{\gamma}_0\| = O(\alpha_n)$ ,  $\hat{\theta}_i(\boldsymbol{\gamma})$  satisfies

$$\nabla_{\boldsymbol{\theta}} L_i^H(\hat{\theta}_i(\boldsymbol{\gamma}), \boldsymbol{\gamma}) = 0 \quad (\text{A.7})$$

for all  $i$ , with probability tending to 1. Moreover, by the Implicit Function Theorem,  $\hat{\theta}_i(\boldsymbol{\gamma})$  is a smooth function of  $\boldsymbol{\gamma}$  in this neighborhood of  $\boldsymbol{\gamma}_0$ . Furthermore, we can establish that

$$\max_{1 \leq i \leq n} \sup_{\boldsymbol{\gamma}: \|\boldsymbol{\gamma} - \boldsymbol{\gamma}_0\| \leq \alpha_n} \|\hat{\theta}_i(\boldsymbol{\gamma}) - \theta_i^*\| = \tilde{O}(\max\{\sqrt{\log n m}^{-1/2}, \alpha_n\}). \quad (\text{A.8})$$

We then proceed to prove (23). By a Taylor series expansion of  $L^P(\boldsymbol{\gamma})$ ,

$$\begin{aligned} L^P(\boldsymbol{\gamma}_0 + \alpha_n \boldsymbol{\delta}) - L^P(\boldsymbol{\gamma}_0) &\approx \alpha_n \boldsymbol{\delta}^T \left( \frac{\partial \boldsymbol{\beta}}{\partial \boldsymbol{\gamma}} \right)^T \frac{dL^P(\boldsymbol{\beta}_0)}{d\boldsymbol{\beta}} + \frac{\alpha_n^2}{2} \boldsymbol{\delta}^T \left( \frac{\partial \boldsymbol{\beta}}{\partial \boldsymbol{\gamma}} \right)^T \frac{d^2 L^P(\boldsymbol{\beta}_0)}{d\boldsymbol{\beta} d\boldsymbol{\beta}^T} \frac{\partial \boldsymbol{\beta}}{\partial \boldsymbol{\gamma}} \boldsymbol{\delta} \\ &= \alpha_n \boldsymbol{\delta}^T \mathbf{C}^T \frac{dL^P(\boldsymbol{\beta}_0)}{d\boldsymbol{\beta}} + \frac{\alpha_n^2}{2} \boldsymbol{\delta}^T \mathbf{C}^T \frac{d^2 L^P(\boldsymbol{\beta}_0)}{d\boldsymbol{\beta} d\boldsymbol{\beta}^T} \mathbf{C} \boldsymbol{\delta}, \end{aligned} \quad (\text{A.9})$$

where the sign  $\approx$  means that the difference between the expression on the left and right sides of (A.9) is of a smaller order than the right side of (A.9), and hence can be ignored asymptotically. The approximation error in the above expansion can be controlled uniformly in  $\boldsymbol{\delta}$ . To justify this, and similar approximations, throughout we use the Hoeffding and Bernstein inequalities, without explicitly referring to them. The key fact we need is that the expected value of  $\mathbf{C}^T (d^2 L^P(\boldsymbol{\beta}) / d\boldsymbol{\beta} d\boldsymbol{\beta}^T) \mathbf{C}$  at  $\boldsymbol{\beta}_0$  is a positive definite matrix and is well-conditioned. This allows us to prove (23) and obtain a rate of convergence for  $\hat{\boldsymbol{\beta}}$ .

Based on the derivations in Section S.3.1 of the Supplementary Material, the following expressions are valid for  $i = 1, \dots, m$ :

$$\frac{d}{d\boldsymbol{\beta}} L_i^P(\boldsymbol{\beta}) = \nabla_{\boldsymbol{\beta}} L_i^H(\hat{\theta}_i(\boldsymbol{\beta}), \boldsymbol{\beta}); \quad (\text{A.10})$$

$$\frac{d^2}{d\boldsymbol{\beta}d\boldsymbol{\beta}^T}L_i^P(\boldsymbol{\beta})=\nabla_{\boldsymbol{\beta}\boldsymbol{\beta}^T}L_i^H(\hat{\boldsymbol{\theta}}_i(\boldsymbol{\beta}),\boldsymbol{\beta})-\nabla_{\boldsymbol{\beta}\boldsymbol{\theta}^T}L_i^H(\hat{\boldsymbol{\theta}}_i(\boldsymbol{\beta}),\boldsymbol{\beta})\left[\nabla_{\boldsymbol{\theta}\boldsymbol{\theta}^T}L_i^H(\hat{\boldsymbol{\theta}}_i(\boldsymbol{\beta}),\boldsymbol{\beta})\right]^{-1}\nabla_{\boldsymbol{\theta}\boldsymbol{\beta}^T}L_i^H(\hat{\boldsymbol{\theta}}_i(\boldsymbol{\beta}),\boldsymbol{\beta}).$$

(A.11)

Based on the derivation in Section S.4.2 of the Supplementary Material, we have

$$\hat{\boldsymbol{\theta}}_i(\boldsymbol{\beta}_0)-\boldsymbol{\theta}_i^*=W_i^*(\boldsymbol{\beta}_0)^{-1}p_{i,\boldsymbol{\theta}}-W_i^*(\boldsymbol{\beta}_0)^{-1}\Psi^{-1}\boldsymbol{\theta}_i^*+W_i^*(\boldsymbol{\beta}_0)^{-1}P_{i,\boldsymbol{\theta}\boldsymbol{\theta}^T}W_i^*(\boldsymbol{\beta}_0)^{-1}p_{i,\boldsymbol{\theta}}+r_{2,i}, \quad (\text{A.12})$$

where  $r_{2,i}$  is negligible and the terms  $W_i^*(\boldsymbol{\beta}_0)$ , and  $p_{i,\boldsymbol{\theta}}$  and  $P_{i,\boldsymbol{\theta}\boldsymbol{\theta}^T}$  are as defined in Section S.4.5.

Next, from the derivation in Section S.4.3, we have the expansion

$$\frac{d}{d\boldsymbol{\beta}}L_i^P(\boldsymbol{\beta}_0)=V_i^{(1)}(\boldsymbol{\beta}_0)+V_i^{(2)}(\boldsymbol{\beta}_0)+r_{4,i}, \quad (\text{A.13})$$

where  $V_i^{(1)}$  and  $V_i^{(2)}$ , defined in (S.44) and (S.45), contribute primarily to the asymptotic variance and asymptotic bias, respectively, and  $r_{4,i}$  is a negligible remainder term. Further calculations, detailed in Section S.4.5, allow us to conclude that

$$\frac{1}{m_i}\frac{d^2}{d\boldsymbol{\beta}d\boldsymbol{\beta}^T}L_i^P(\boldsymbol{\beta}_0)=\Xi^{1/2}(a_i,\boldsymbol{\theta}_i^*,\boldsymbol{\beta}_0)+\tilde{O}\left(\max\left\{\frac{\lambda}{n},\sqrt{\frac{\log n}{m}}\right\}\right), \quad (\text{A.14})$$

By the definition of  $\tilde{G}(a_i, \boldsymbol{\theta}_i, \boldsymbol{\beta})$  in (18), the empirical Fisher information matrix satisfies

$$F_n(\boldsymbol{\gamma}_0):=\frac{1}{N_n}\sum_{i=1}^n\mathbf{C}^T\frac{d^2}{d\boldsymbol{\beta}d\boldsymbol{\beta}^T}L_i^P(\boldsymbol{\beta}_0)\mathbf{C}=\frac{1}{N_n}\sum_{i=1}^nm_i\tilde{G}(a_i,\boldsymbol{\theta}_i^*,\boldsymbol{\gamma}_0)+\tilde{O}\left(\max\left\{\frac{\lambda}{n},\sqrt{\frac{\log n}{m}}\right\}\right).$$

(A.15)

By (A.15), and the fact that  $\mathcal{G}(\boldsymbol{\gamma})$ , defined in (19), is positive definite at  $\boldsymbol{\gamma}_0$ , we conclude that for a given  $c > 0$ , with probability at least  $1 - n^{-c}$ , the inverse of  $F_n(\boldsymbol{\gamma}_0)$  exists and the maximum eigenvalue of the inverse is bounded.

Combining (A.15) with (A.13) and (A.9), and using the fact that  $\lambda = o(\sqrt{n})$ , we obtain (23) with  $a_n = c \max\{(\log n)^{1/2}(n\underline{m})^{-1/2}, \underline{m}^{-1}\}$  for some suitable positive constant  $c$ . This establishes that there exists a root  $\hat{\boldsymbol{\gamma}}$  of  $\frac{d}{d\boldsymbol{\gamma}}L^P(\boldsymbol{\gamma})=0$  satisfying  $\|\hat{\boldsymbol{\gamma}} - \boldsymbol{\gamma}_0\| = O_P(a_n)$ . Finally, we expand the equation  $\frac{d}{d\boldsymbol{\gamma}}L^P(\hat{\boldsymbol{\gamma}})=0$  around  $\boldsymbol{\gamma}_0$  to obtain

$$\hat{\boldsymbol{\gamma}} - \boldsymbol{\gamma}_0 = - \left( \frac{1}{N_n} \sum_{i=1}^n \mathbf{C}^T \frac{d^2}{d\boldsymbol{\beta}d\boldsymbol{\beta}^T} L_i^P(\boldsymbol{\gamma}_0) \mathbf{C} \right)^{-1} \left( \frac{1}{N_n} \sum_{i=1}^n \mathbf{C}^T \frac{d}{d\boldsymbol{\beta}} L_i^P(\boldsymbol{\gamma}_0) \right) + O_P(\alpha_n^2 \log n). \tag{A.16}$$

This concludes the proof of Theorem 1 once we isolate the leading terms in  $\frac{d}{d\boldsymbol{\beta}}L_i^P(\boldsymbol{\gamma}_0)$  (namely, (S.44) and (S.45)) and use the fact that  $(a_i, \boldsymbol{\theta}_i^*)$  are i.i.d.

### A.3 Proof of Theorem 2

The proof follows from a careful treatment of (A.16). We move the contribution of the bias term  $V_i^{(2)}(\boldsymbol{\beta}_0)$  in (S.45) to the side of  $\hat{\boldsymbol{\gamma}} - \boldsymbol{\gamma}_0$  in (A.16), and use the representations (S.37), (S.38), (S.39), and (S.42), taking appropriate conditional expectations to derive the form of the asymptotic bias  $b_n(\boldsymbol{\gamma}_0)$ . Next we use the representation (A.13) of  $\frac{d}{d\boldsymbol{\beta}}L_i^P(\boldsymbol{\beta}_0)$ , and the expression of the variance term  $V_i^{(1)}(\boldsymbol{\beta}_0)$  in (S.44), and a version of martingale central limit theorem, through the independence of  $(a_i, \boldsymbol{\theta}_i^*, (\varepsilon_{ij})_{j=1}^{m_i})$  across  $i$ , to conclude that  $V_i^{(1)}(\boldsymbol{\beta}_0)$  has an asymptotic Gaussian limit. The condition **AS'** ensures that the remainder terms are  $o_P(1)$ . The nonsingularity of  $\mathcal{G}(\boldsymbol{\gamma}_0)$  combined with (A.15) concludes the derivation.

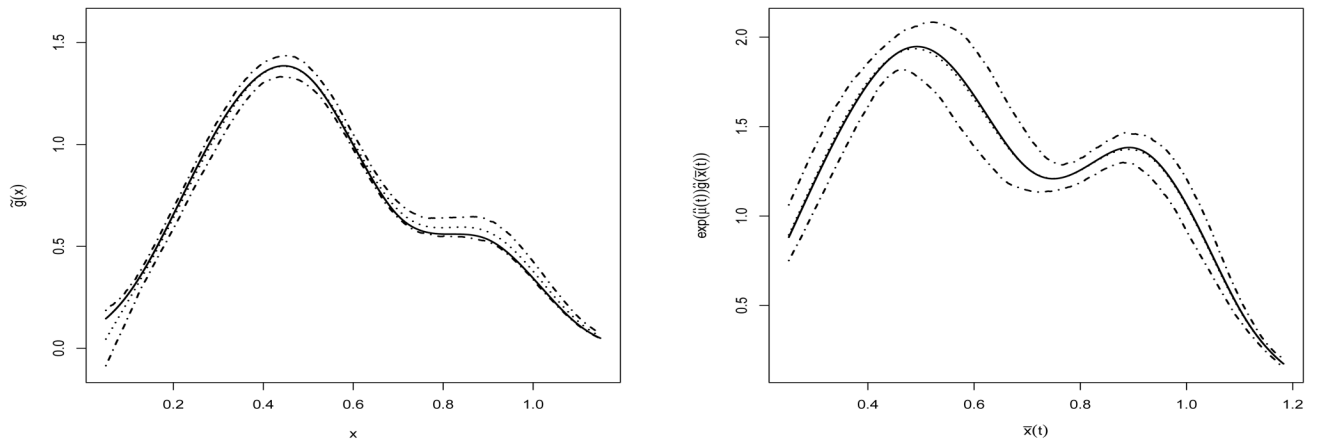


**Figure 1.** Simulation with “Two-peak” gradient function  $g$  and linear  $Z(\cdot, \theta_i)$ : dense case with  $\mu_\theta = (0, 2)^T$  and  $\sigma_e = 0.01$ . **Left panel:** X-axis:  $x$ ; Solid line: true  $g(x)$ ; Dotted line: point-wise mean of  $\hat{g}(x) = s_\beta \hat{g}(x)$ ; Dash-dotted line: point-wise 5% and 95% percentiles of  $\hat{g}(x)$ . **Right panel:** X-axis: mean of  $\bar{X}(t)$ ; Solid line: point-wise mean of  $e^{\mu(t)} g(\bar{X}(t))$ ; Dotted line: point-wise mean of  $e^{\hat{\mu}(t)} \hat{g}(\bar{X}(t))$ ; Dash-dotted line: point-wise 5% and 95% percentiles of  $e^{\hat{\mu}(t)} \hat{g}(\bar{X}(t))$ .



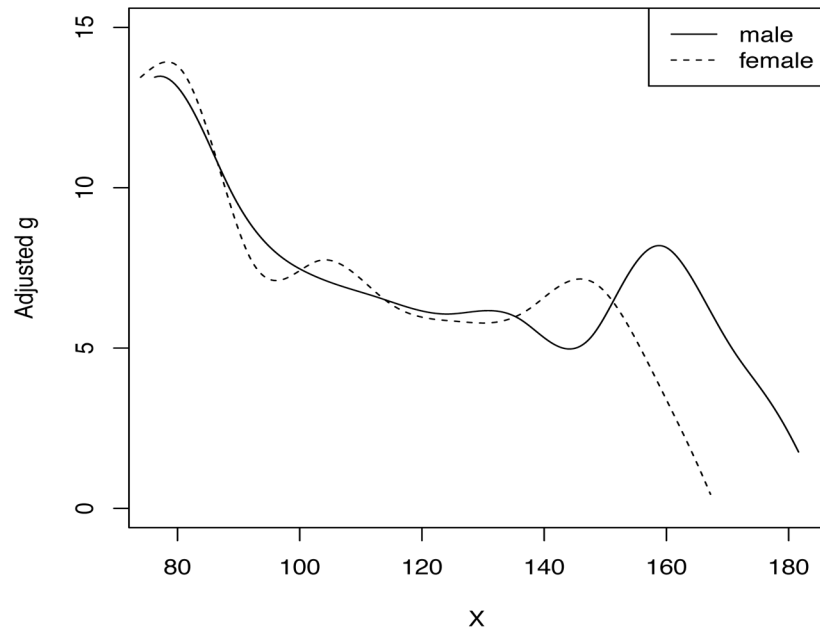


**Figure 2.** Berkeley growth data. Fitted gradient  $e^{\mathcal{Z}(t)\hat{\boldsymbol{\mu}}\boldsymbol{\theta}}g(\bar{X}(t))$  against  $\bar{X}(t)$  under quadratic subject-specific effects ( $p=3$ ) for female group (dashed line) and male group (solid line).

Simulation with “Two-peak” baseline gradient function  $\mathcal{g}$  and linear ( $p = 2$ )  $Z(\cdot, \theta_j)$ 's, with  $M = 30$  cubic B-spline basis functions used in fitting,  $\widehat{CV}$  used for selection of  $\lambda_{\beta}$ .

**Table 1**

Sampling rate	$\mu_2$	$\sigma_e$	Mean(ISE)	SD(ISE)	Median(ISE)	MAD(ISE)
$ISE(\hat{\beta})$						
sparse	0	0.01	0.001801	0.001238	0.001558	0.001053
	2	0.01	0.004457	0.002762	0.003956	0.002453
dense	2	0.01	0.001500	0.001588	0.001024	0.000810
	2	0.02	0.002730	0.002371	0.001935	0.001319
$1000 \times ISE(\hat{X})$						
sparse	0	0.01	0.053307	0.034124	0.049418	0.014179
	2	0.01	0.084852	0.701658	0.050115	0.013050
dense	2	0.01	0.039038	0.700262	0.006779	0.001343
	2	0.02	0.022918	0.005040	0.022217	0.004702